

# Single Pixel Compressive Imaging of Laboratory and Natural Light Scenes

Stephen J. Olivas,<sup>1</sup> Yaron Rachlin,<sup>2,3</sup> Lydia Gu,<sup>2,4</sup> Brian Gardiner,<sup>2</sup>  
Robin Dawson,<sup>2</sup> Juha-Pekka Laine<sup>2</sup> and Joseph E. Ford<sup>1</sup>

<sup>1</sup>Photonic Systems Integration Laboratory, Electrical Engineering Department  
University of California at San Diego, 9500 Gilman Dr., La Jolla, CA 92093, USA.

<sup>2</sup>The Charles Stark Draper Laboratory, Inc.,  
555 Technology Square, Cambridge, Massachusetts 02139, USA.

<sup>3</sup>Currently with MIT Lincoln Laboratory,  
244 Wood Street, Lexington, MA 02420-9108 USA.

<sup>4</sup>Currently with Cogito Health, 7 Water Street, Suite 400, Boston, MA 02109 USA.

Contact: Stephen J. Olivas tel: 858.822.4406 fax: 858.534.1225 email:sjolivas@ucsd.edu

**Abstract:** We evaluate the performance of a compressive imager using multiple basis sets on monochromatic, color and infrared natural light scenes, and compare the results to a camera with the same number of (conventional pixel) measurements.

© 2013 Optical Society of America

**OCIS codes:** 110.0110 Imaging systems, 100.0100 Image processing and 110.1758 Computational imaging.

Traditional cameras capture one measurement per pixel then discard much of the data during compression, whereas compressive imaging (CI) systems acquire comparably fewer spatially filtered scene measurements from which to reconstruct an image [1]. This eliminates processing unused data, making CI more efficient. Several system designs have been considered [2] as well as custom sensor implementations [3]. CI is based the idea that by sampling an image with random basis set, the sparsest solution can be found. We explore this mode of operation as well as one in which lower spatial frequencies are selectively sampled, making it tailored to the statistical distribution of natural images [4], given by  $S(f) = f^{-\gamma}$ , where  $1.8 < \gamma < 2.3$ . To do so, we assembled and characterized a single-pixel CI system [5, 6] (Fig. 1) and compared it to a conventional imager using both laboratory and outdoor natural light scenes.

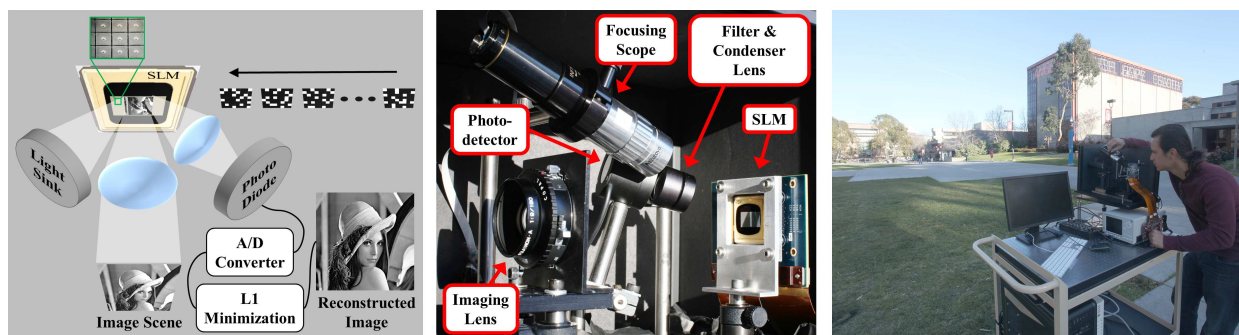


Fig. 1. (Left) System schematic: a scene is imaged onto a spatial light modulator (SLM) which redirects the weighted scene energy to a photodiode for measurement acquisition. (Center) Photo of the CI system. (Right) Photo of CI system taking outdoor natural light images.

## 1. System Design and Configuration

A computer running Digital Light Innovation's Accessory Light-modulator Package (ALP) software was used to upload previously generated PNG transform basis image files to the Discovery D4100 controller board via a USB 2.0 link, which in turn controls the Texas Instruments digital micro-mirror device (DMD) chip. A Newport Optics Corporation photo-detector 918D-SL was used to measure light intensity collected from the DMD and send it to a Newport

power meter 1936-C which was sampled using a National Instruments data acquisition card PCIe-6363 in the desktop computer. The sampling of the basis coefficients was synchronized with the displaying of each basis projection.

The input scene is imaged onto the DMD using a Fujinon F/9 double Gauss Copal lens,  $f=180\text{mm}$  while a condenser lens directs the optical energy from the DMD onto a single element photo-detector. Each basis function PNG file's resolution is  $1920\times 1080$ , corresponding to the DMD specifications, with the actual transforms occupying the center  $1024\times 1024$  mirrors for a total of 1,048,576 mirrors. This determines the maximum resolution of the system. The image reconstruction problem posed by the CI system is of the form  $b = Ax + z$ , where  $A$  is the sampling basis set,  $z$  is the noise term,  $b$  is the measured basis coefficients and  $x$  is the image we reconstruct. We used the NESTA software package for quick and accurate reconstruction [7] which took less than 1 minute for each image.

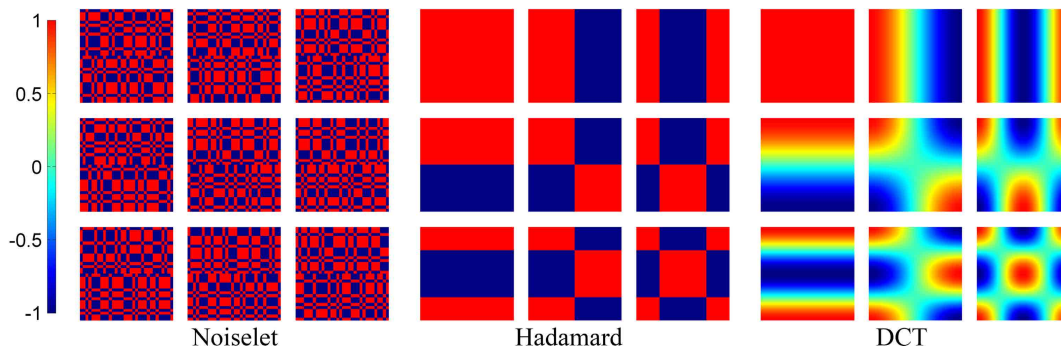


Fig. 2. Basis transform sets used to take measurements with the CI system.

We tested the noiselet, Hadamard-Walsh (HW) and the discrete cosine transform (DCT) to characterize system performance (Fig. 2). The noiselet transform ( $1\text{-bit}$ ) was chosen as a representative measurement basis for CI since it is incoherent with impulses and Fourier basis [1]. The HW ( $1\text{-bit}$ ) and DCT ( $8\text{-bit}$ ) transforms were used to specifically target low spatial frequencies. We imaged two indoor chrome on glass transparencies (USAF 1951 resolution target and standard Lena test image), see Fig. 3, which were back illuminated using a 10 W white-light four element (Seoul Semiconductor model number P7) LED and diffusive screen. A Canon 5D Mark II camera with resolution superior to the CI system served to acquire ground truth images. For these monochrome images there was 11.91 mW of power at the camera lens. During these indoor tests, stray light was well controlled and its effects negligible. Outdoor daylit experimental data was captured using RGB optical filters to create color images. The RGB color filters had a center wavelength of 450 nm, 550 nm and 650 nm each with a bandwidth of 70 nm. The outdoor power reading measured using the Newport power meter was 8.9 W and with the respective filters present was 484 mW, 623 mW and 969 mW. Contrast was limited to 20dB in part by the DMD chip.

## 2. Experimental Result and Discussion

Conventional 1.04MPix ground truth images are shown in the left column of Fig. 3. These images are binned to 10,486 pixels and upsampled back to their original size (second column). They serve as a comparison with the compressive images reconstructed using 10,486 measurements (three columns to the right). Image acquisition with the noiselet and HW images took about 7 minutes, while with the DCT took about 20 minutes. This is due to the larger memory needed to store and transfer the  $8\text{-bit}$  DCT patterns. The noiselet reconstructions seem to be data starved and the overall structure was less formed. Both the DCT and HW produced more accurate reconstructions when compared to the noiselet, due in part to selective sampling low spatial frequencies. The DCT reconstructions exhibited ringing artifacts near object edges. The HW transform produced the most appealing compressive images. The long exposure time of the CI system made illumination changes of the daylit scene significant, evident in the color channel differences of the outdoor scene. All compressive images were less smooth but had substantially comparable resolution when compared to conventional images. Overall the CI system performed as expected, producing comparable images to a conventional camera when both are limited to the same amount of data, however the system in general performs with impractical exposure times. We concluded that the HW transform was the best representation for general-purpose compressive imaging. We characterized and validated the CI system with various transforms and under different lighting conditions.

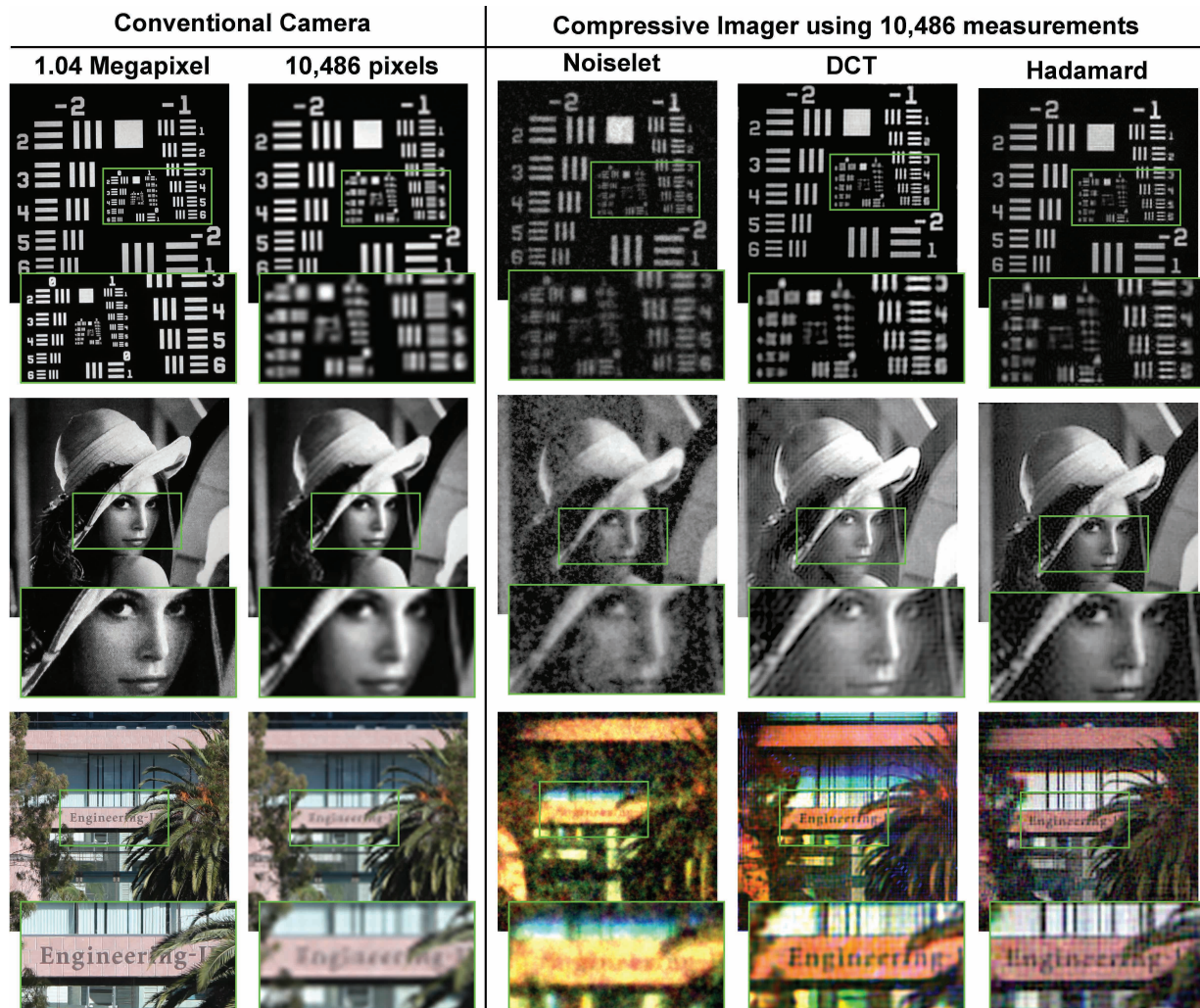


Fig. 3. Comparison of images acquired using a conventional camera and a compressive imager.

## References

1. E.J. Candès and M.B. Wakin, "An Introduction To Compressive Sampling," *IEEE Signal Processing Magazine*, **25** (2), 21 -30 (2008).
2. M.A. Neifeld and J. Ke, "Optical architectures for compressive imaging," *Appl. Opt.*, **46** (22), 5293–5303 (2007).
3. R. Robucci, Leung Kin Chiu, J. Gray, J. Romberg, P. Hasler, and D. Anderson, "Compressive sensing on a CMOS separable transform image sensor," *IEEE International Conference on Acoustics, Speech and Signal Processing*, 2008. ICASSP 2008, 5125–5128 (2008).
4. D.L. Ruderman, "Origins of Scaling in Natural Images," *Vision Research*, **37** (23), 3385–3398 (1997).
5. M.F. Duarte, M.A. Davenport, D. Takhar, J.N. Laska, Ting Sun, K.F. Kelly and R.G. Baraniuk, "Single-Pixel Imaging via Compressive Sampling," *IEEE Signal Processing Magazine*, **25** (2), 83 -91 (2008).
6. L. McMackin, M.A. Herman, B. Chatterjee and M. Weldon, "A high-resolution SWIR camera via compressed sensing," *Proc. SPIE 8353, Infrared Technology and Applications XXXVIII*, 835303-835313 (2012).
7. S. Becker, J. Bobin and E. Candès, "NESTA: A Fast and Accurate First-Order Method for Sparse Recovery," *SIAM Journal on Imaging Sciences*, **4** (1), 1-39 (2011).
8. S. Olivas, Y. Rachlin, L. Gu, B. Gardiner, R. Dawson, J.P. Laine and J.E. Ford, "Characterization of a Compressive Imaging System using Laboratory and Natural Light Scenes," *Appl. Opt.*, (2013, in review).